Supporting Information

Tunable Rhenium–Ceria–Zirconia Catalysts for Efficient Deoxydehydration of C_6 Polyols: Lattice Engineering Enables High Muconate Yield

Gukhee Yim,†[a] Hyunwoo Choi,†[a] Hyeonjeong Son,†[a] Juhye Park,[a] Ahyun Jeon,[a] Youngran Seo,*[a] and Dongwon Yoo*[a,b]

[a] Department of Chemical and Biological Engineering, and Institute of Chemical Processes, Seoul National University, Seoul 08826, Republic of Korea

[b] Center for Nanoparticle Research, Institute for Basic Science (IBS), Seoul 08826, Republic of Korea

* Corresponding authors: youngran02@snu.ac.kr; dwyoo@snu.ac.kr

† Contributed equally

Table of Contents

1. General Information

All reagents were purchased from commercial sources (Alfa Aesara and Sigma Aldrich) without further treatment. Thin-layer chromatography was run on SiO_2 plate, then visualized under UV light (254 nm) followed by a potassium permanganate staining solutions. Column chromatography was performed on silica gel 60.

^1H NMR (400 MHz) and ^{13}C NMR (100 MHz) spectra were obtained with a Bruker 400 AVANCE at Seoul National University Chemical Biological Engineering Research Facilities. All chemical shifts are referenced to residual non-deuterated solvent signals (note: $CDCl_3$ reference at 7.26 and 77.16 ppm, DMSO-d_6 referenced at 2.50 and 39.52 ppm, MeOD-d_4 referenced at 3.31 and 49.00 ppm, respectively for ^1H NMR and ^{13}C NMR). ^1H NMR were presented as following: chemical shifts (δ, ppm), multiplicity (d = doublet, t = triplet, dd = doublet of doublets, m = multiplet), coupling constant (Hz) and integration.

The morphology of the materials was observed with field emission-transmission electron microscopy (FE-TEM, JEM-F200(TFEG)), at National Center for Inter-University Research Facilities (NCIRF) of Seoul National University. 200 kV was used for acceleration voltage. Also, elemental mapping images from Energy dispersive X-ray spectroscopy were obtained from the STEM mode. High-performance X-ray photoelectron spectrometer (XPS) system (Thermo Fisher Scientific) was analyzed using Al-Kα radiation (1486.6 eV) at the Busan center of Korea Basic Science Institute (KBSI). Inductively Coupled Plasma mass spectrometer (ICP-AES) analysis was conducted with ICP-730ES at the National Instrumentation Center for Environmental Management (NICEM) at Seoul National University. X-ray diffraction (XRD) patterns were conducted by a Bruker D8 Advance, 2020 (multi-purpose XRD, Cu Kα radiation) at Research institute of advanced materials (RIAM) in Seoul National University. Electron paramagnetic spectroscopy was analyzed with JEOL (JES-X320) at 77 K in Kangwon National University.

2. Experimental Procedure

2.1. Synthesis of CeO_2 nanorod[1]

CeO_2 nanorods were synthesized through a hydrothermal method. Briefly, $Ce(NO_3)_3 \cdot 6H_2O$ (1.74 g, 4.0 mmol) was dissolved in 9.3 mL distilled water and added to aqueous solution of 6 M NaOH (70 mL), and stirred for 30 mins at room temperature. The mixture was transferred to a 100 mL Teflon bottle, placed in a stainless-steel vessel autoclave, and the autoclave was sealed tightly. Hydrothermal treatment was carried out by placing the autoclave in a temperature-regulated oven and maintaining it at 100 ℃ for 24 h. After cooled to room temperature, the precipitates were separated by centrifugation, washed with distilled water and ethanol, and dried at 60 ℃ overnight.

2.2. Synthesis of $Ce_xZr_{1-x}O_2$ mixed oxide

CeO_2 nanorod (400 mg) were dispersed in 60 mL distilled water containing 1, 2, or 3 mmol of $ZrO(NO_3)_2 \cdot H_2O$, and sonicated for 1 h. The suspension was then subjected to hydrothermal treatment at 180 ℃ for 10 h. The precipitate was washed with ethanol and dried at 100 ℃ overnight. The resulting residue was gently grinded with mortar and transferred to alumina crucible. Then, it was heated to 600 ℃ under air with a ramping rate of 10 ℃/min and maintained at 600 ℃ for 6 h. The as-prepared catalysts were denoted as $Ce_{0.5}Zr_{0.5}O_2$, $Ce_{0.3}Zr_{0.7}O_2$, and $Ce_{0.2}Zr_{0.8}O_2$, respectively, corresponding to the initial precursor ratios.

2.3. Synthesis of $Re/Ce_xZr_{1-x}O_2$

$Ce_xZr_{1-x}O_2$ (200 mg) was subjected to the NH_4ReO_4 aqueous solution (0.14 M, 400 μL), and sonicated for 15 mins. The resulting mixture was dried at 100 ℃ overnight. The dried powders were gently grinded with mortar and transferred to alumina crucible. Then it was heated to 500 ℃ under air with a ramping rate of 10 ℃/min and maintained at 500 ℃ for 3 h.

2.4. Synthesis of dibutyl galactarate (1)

Galactaric acid (1.05 g, 5 mmol) and *p*-TsOH·H_2O (48 mg, 0.05 eq.) were dissolved in n-butanol (17 mL). The reaction mixture was stirred at 90 ℃ for 48 h under Ar atmosphere. After the reaction, the reaction mixture was filtered and the filtrate was concentrated under reduced pressure, and white solid was obtained. The white solid was precipitated with ethyl acetate, and obtained dibutyl galactarate with 61% yield.

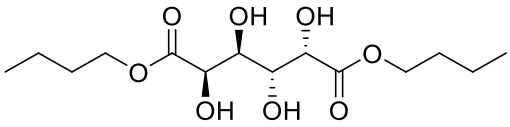

Pearl white solid, ^{1}H NMR(400 MHz, DMSO-d_6): δ= 4.92 (d, J = 7.9 Hz, 2H), 4.82-4.80 (m, 2H), 4.29 (d, J=7.80, 2H), 4.11-4.01 (m, 4H), 3.79-3.77 (m, 2H), 1.58-1.52 (m, 4H), 1.36-1.28 (m, 4H), 0.89 (t, J = 7.4 Hz, 6H); ^{13}C NMR (100 MHz, DMSO-d_6); δ= 173.7, 71.3, 70.2, 63.8, 30.3, 18.6, 13.6

The above analytic data is in agreement with previously published data.[2]

2.5. DODH reaction with $Re/Ce_xZr_{1-x}O_2$

Dibutyl galactarate (0.5 mmol, 161 mg) and the catalyst (Re 5 mol%, 93 mg) were placed in a vial and dried under reduced pressure for 20 mins before reaction. The vacuum-dried reagents were transferred to oven-dried two-neck round bottom flask with Dean-Stark, followed by the addition of n-butanol (19 mL). The reaction mixture was vigorously stirred at 145 ℃ for 12 h under Ar atmosphere. After the reaction, the reaction mixture was filtered with dichloromethane and the filtrate was concentrated under reduced pressure. The product was isolated by silica gel column chromatography with DCM/MeOH=10/1.

1,6-Dibutyl (*E*,*E*)-2,4-hexadienedioate (2)

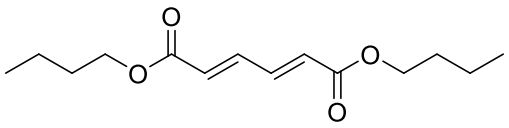

Transparent solid, ^{1}H NMR (400 MHz, $CDCl_3$): δ= 7.30 (dd, *J* = 3.1 Hz, *J* = 11.4 Hz, 2H), 6.20 (dd, *J* = 3.1 Hz, *J* = 11.4 Hz, 2H), 4.18 (t, *J* = 6.7 Hz, 4H), 1.70-1.62 (m, 4H), 1.45-1.36 (m, 4H), 0.95 (t, *J* = 7.4 Hz, 6H); ^{13}C (100 MHz, $CDCl_3$) 166.2, 140.9, 128.5, 64.9, 30.8, 19.3, 13.9

The above analytic data is in agreement with previously published data.[3]

Dibutyl (*E*)-4,5-dihydroxyhex-2-enedioate (3)

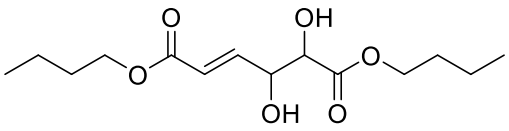

Colorless oil, ^{1}H NMR (400 MHz, MeOD-d_4): δ= 7.03 (dd, *J* = 4.6 Hz, *J* = 15.6 Hz, 1H), 6.11 (dd, *J* = 1.8 Hz, *J* = 15.6 Hz, 1H), 4.59-4.58 (m, 1H), 4.25 (d, *J* = 3.3 Hz, 1H), 4.20-4.13 (m, 4H), 1.69-1.62 (m, 4H), 1.45-1.39 (m, 4H), 0.98-0.94 (m, 6H); ^{13}C (100 MHz, MeOD-d_4) 173.5, 168.0, 148.7, 122.7, 74.8, 73.3, 66.1, 65.4, 31.9, 31.8, 20.2, 20.1, 14.4, 14.0

3. Supplementary Figures

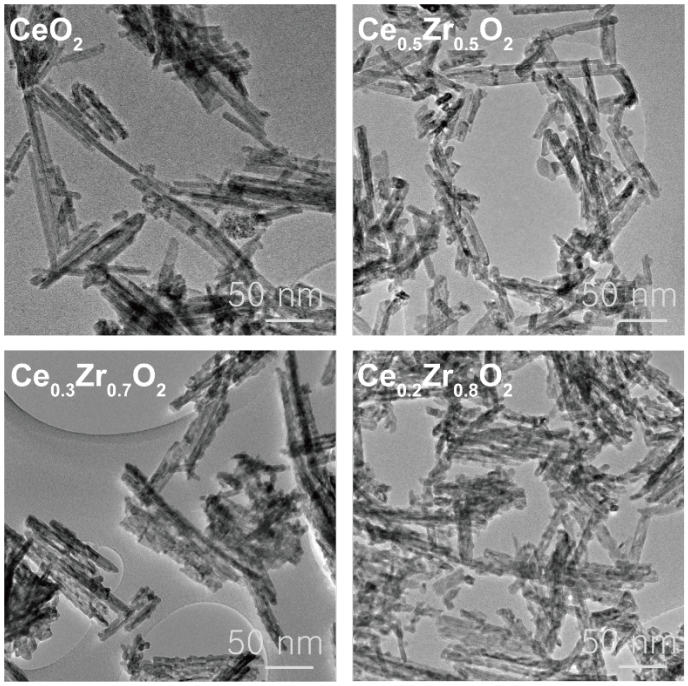

Figure S1. TEM images of $Ce_xZ_{1-x}O_2$.

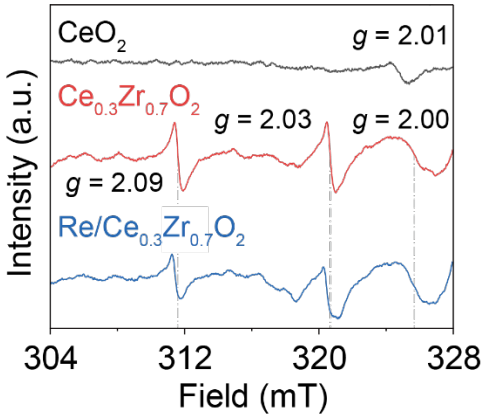

Figure S2. EPR spectra of CeO_2 (black), $Ce_{0.3}Z_{0.7}O_2$ (red), and $Re/Ce_{0.3}Zr_{0.7}O_2$ (blue) measured at 77 K. Several characteristic signals associated with oxygen-vacancy-related defect centers are observed for $Ce_{0.3}Zr_{0.7}O_2$ and $Re/Ce_{0.3}Zr_{0.7}O_2$. A broad signal at $g \approx 2.00$ is assigned to superoxide anions ($O_2^{\bullet-}$), which are known to form in the presence of electron-rich oxygen-vacancy-related sites. The enhanced intensity of this signal for $Ce_{0.3}Zr_{0.7}O_2$ and $Re/Ce_{0.3}Zr_{0.7}O_2$ indicates a higher density of oxygen vacancies. The signal at $g \approx 2.03$ is attributed to Ce^{3+} species associated with oxygen vacancies, while the feature at $g \approx 2.09$ corresponds to paramagnetic defect centers commonly observed in defective oxide lattices.

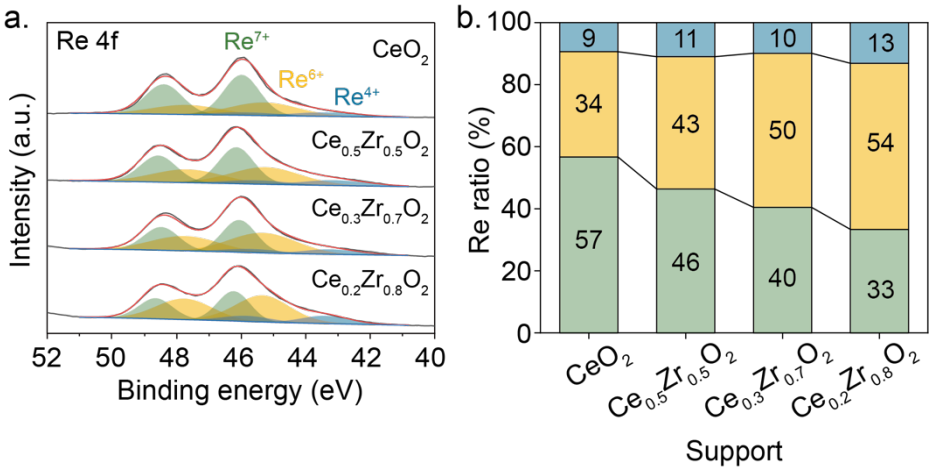

Figure S3. (a) XPS spectra of Re *4f* and (b) ratio of each Re oxidation states (Re^{7+} green, Re^{6+} orange, Re^{4+} blue).

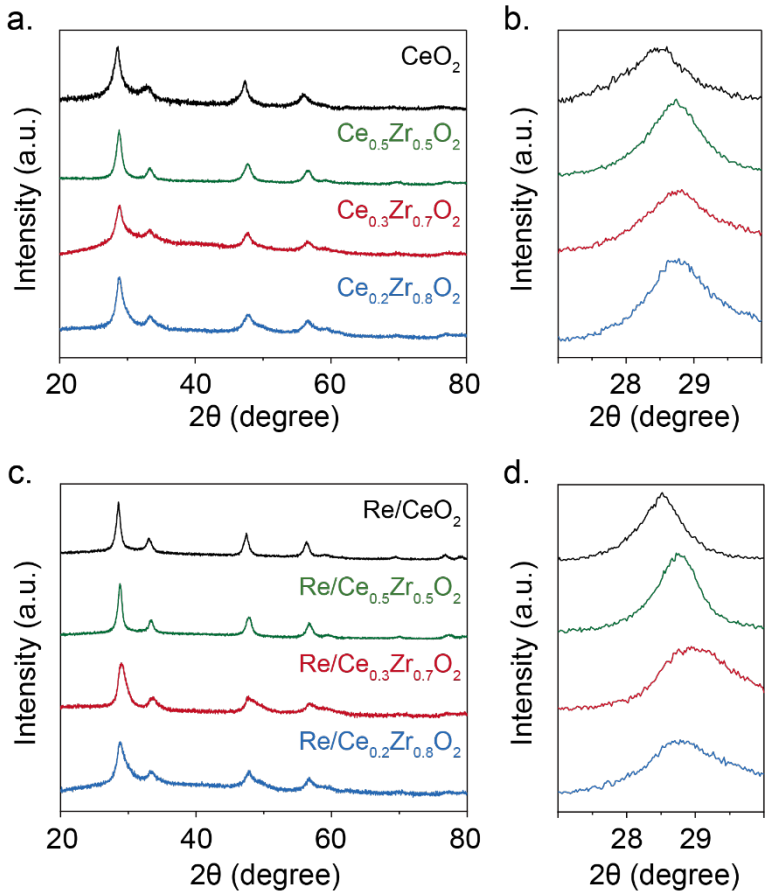

Figure S4. (a) Full XRD spectra of $Ce_xZ_{1-x}O_2$, and its enlarged view of the (111) diffraction region (b). (c) Full XRD spectra of $Re/Ce_xZ_{1-x}O_2$, and its enlarged view of the (111) diffraction region (d).

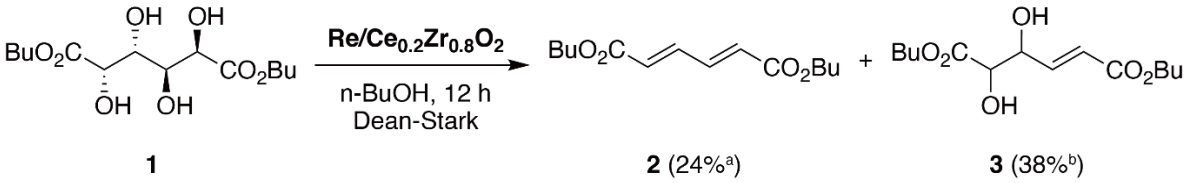

1 **2** (24%[a]) **3** (38%[b])

Scheme S1. Yield of product **2** and intermediate **3** over $Re/Ce_{0.2}Zr_{0.8}O_2$. [a]Isolation yield. [b]Yield determined from crude ^1H NMR using 1,3,5-triisopropylbenzene as an internal standard.

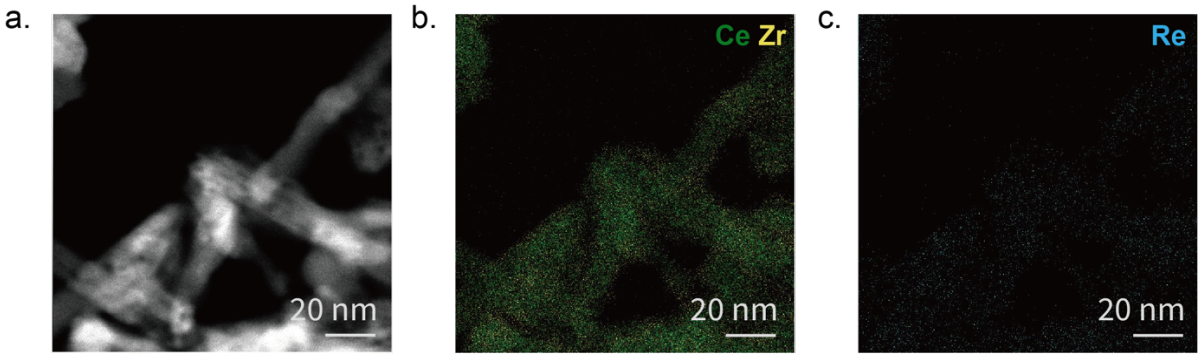

Figure S5. Structural characterization of $Re/Ce_{0.3}Zr_{0.7}O_2$. (a) Secondary electron image (SEI). EDS mapping images of (b) Ce (green) and Zr (yellow) overlay, and (c) Re (blue).

4. Supplementary Tables

Table S1. ICP-AES analysis for Re wt%

Catalyst	1st	2nd	3rd	4th	Averaged (wt%)
Re/CeO_2	4.63	4.98	5.13	-	4.91
$Re/Ce_{0.5}Zr_{0.5}O_2$	5.28	4.99	5.31	-	5.19
$Re/Ce_{0.3}Zr_{0.7}O_2$	5.68	5.61	4.09	3.92	4.82
$Re/Ce_{0.2}Zr_{0.8}O_2$	5.20	5.16	4.91	5.02	5.11

5. NMR Spectra

^{1}H NMR spectrum (400 MHz, DMSO-d_6) of **1**

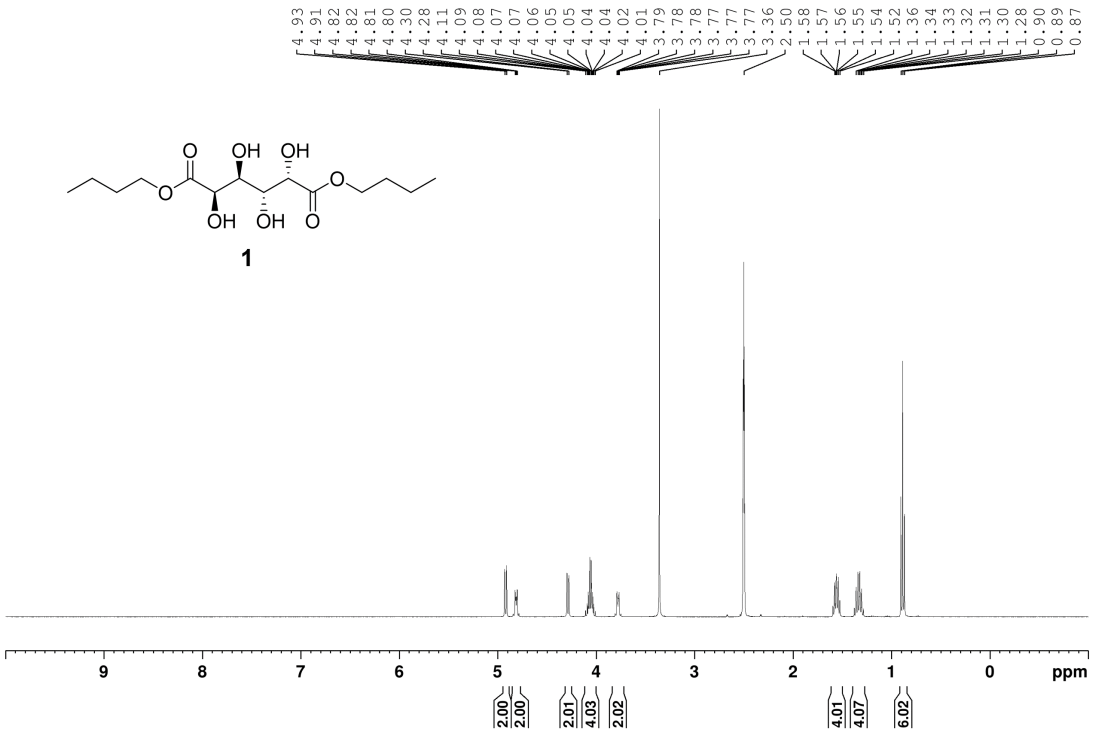

^{13}C NMR spectrum (100 MHz, DMSO-d_6) of **1**

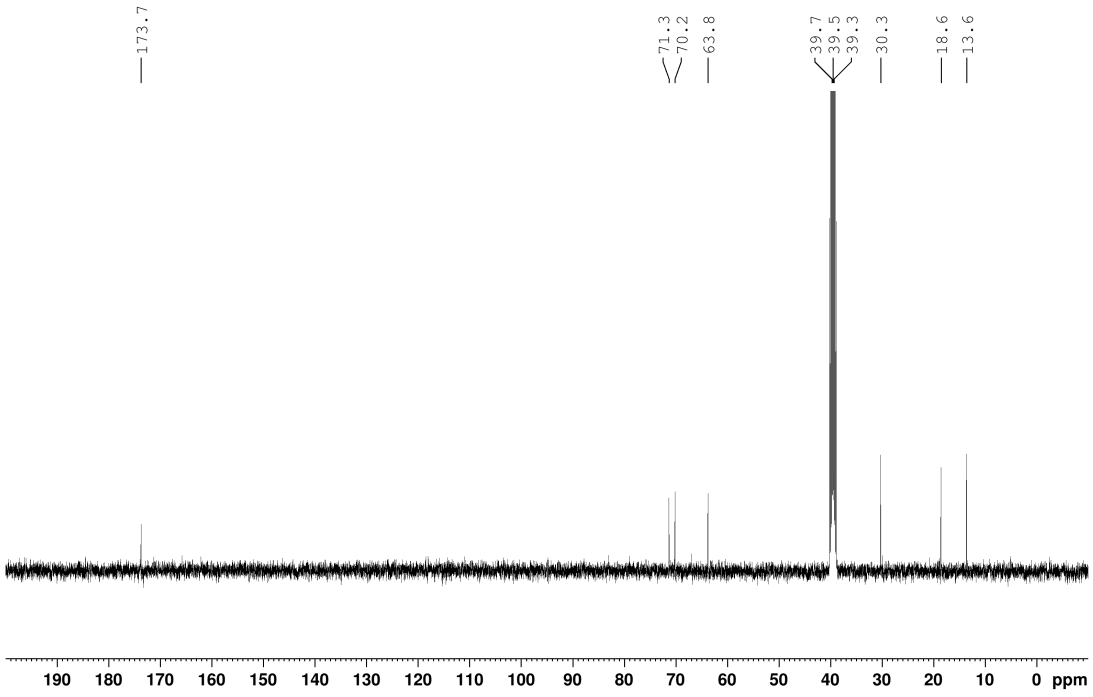

^{1}H NMR spectrum (400 MHz, $CDCl_3$) of **2**

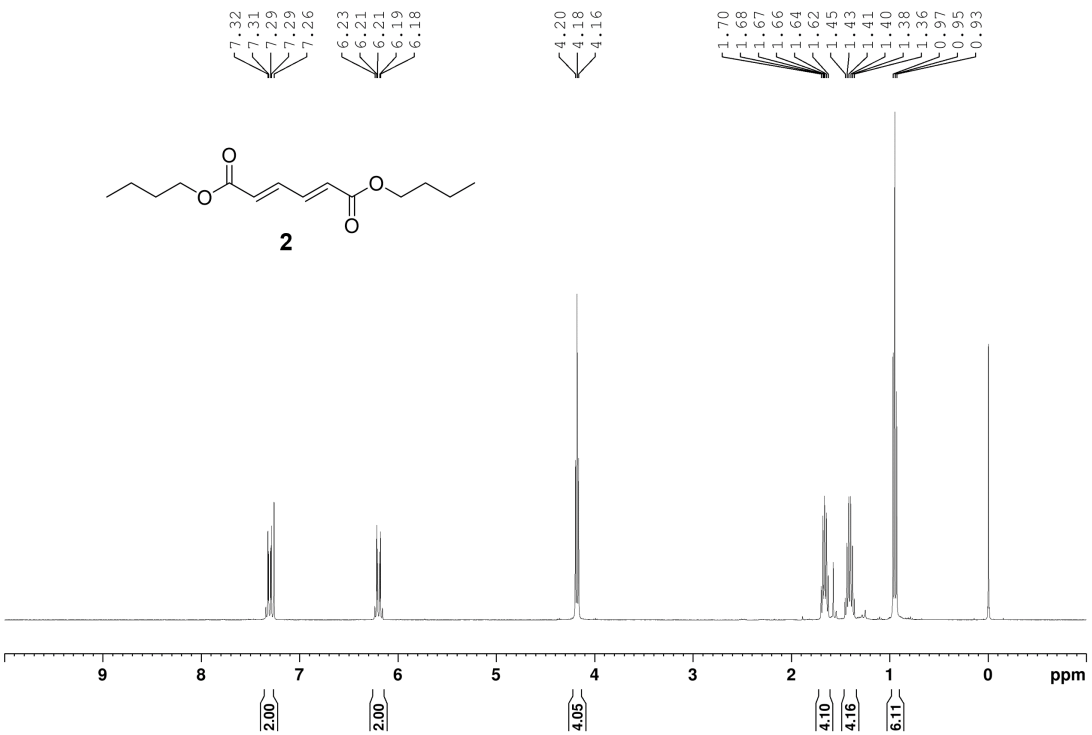

^{13}C NMR spectrum (100 MHz, $CDCl_3$) of **2**

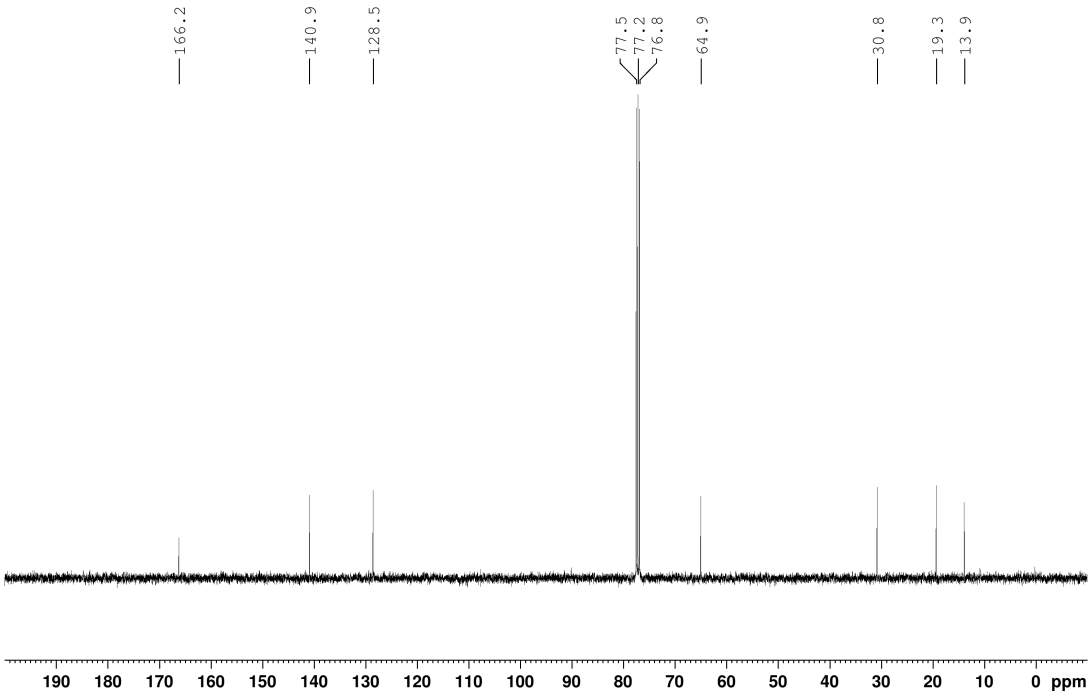

^{1}H NMR spectrum (400 MHz, MeOD-d_4) of **3**

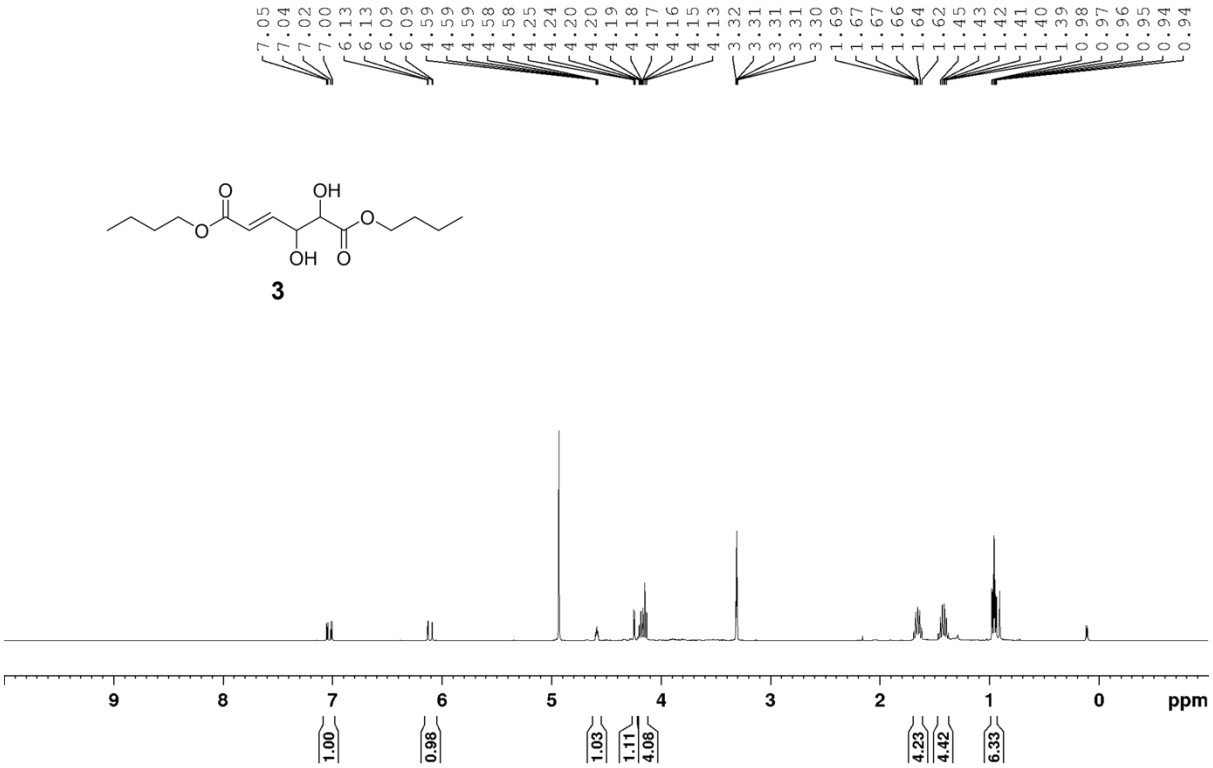

^{13}C NMR spectrum (100 MHz, MeOD-d_4) of **3**

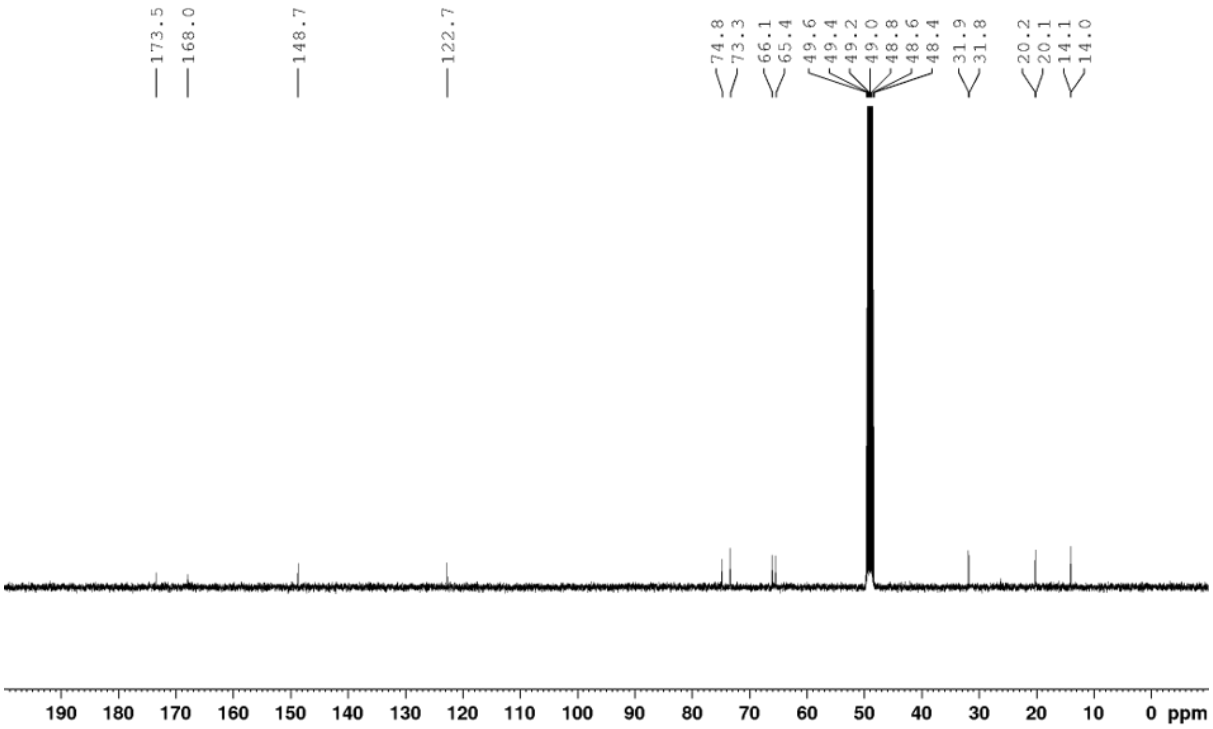

6. References

1. H.-X. Mai, L.-D. Sun, Y.-W. Zhang, R. Si, W. Feng, H.-P. Zhang, H.-C. Liu and C.-H. Yan, *The Journal of Physical Chemistry B*, 2005, **109**, 24380-24385.
2. N. Shin, S. Kwon, S. Moon, C. H. Hong and Y. G. Kim, *Tetrahedron*, 2017, **73**, 4758-4765.
3. T. Zhu, Z. Li, F. Xiao and W.-L. Duan, *Tetrahedron Letters*, 2018, **59**, 3238-3241.